Thesis for the degree of Doctor of Philosophy

Deep Learning Applications

From image analysis to medical diagnosis

Saga Helgadottir

Department of Physics
University of Gothenburg

Gothenburg, Sweden 2021

UNIVERSITY OF GOTHENBURG

Deep Learning Applications
From image analysis to medical diagnosis

Saga Helgadottir
978-91-8009-366-8 (printed)
978-91-8009-367-5 (electronic)

Department of Physics
University of Gothenburg
SE-412 96 Göteborg
Tel: +46 (0)31-7721000 htttp://www.physics.gu.se

Printed by STEMA SPECIALTRYCK AB
Borås, Sweden 2021

Deep Learning Applications

From image analysis to medical diagnosis

Saga Helgadottir
Department of Physics
University of Gothenburg

Abstract

Deep learning is a subcategory of machine learning and artificial intelligence. Instead of using explicit rules to perform a desired task as in standard algorithmic approaches, machine-learning algorithms autonomously learn from data to determine the rules for the task at hand. The idea of deep learning has been around since the 1950s but was for a long time limited by available computational power and amount of training data. Once overcome these problems, in recent years, deep learning has made great advances in solving various problems.

In this thesis, I show how deep learning can be applied in image analysis and medical diagnosis, while outperforming standard algorithmic methods and simpler machine-learning methods. I begin with showing that a convolutional neural network trained with simulated particle images is able to track experimental single particles, even in poor illumination conditions. I then show how this inspired the development of an all-in-one software to design, train and validate deep-learning solutions for digital microscopy, from particle tracking and characterization in 2D and 3D to the segmentation, characterization and counting of biological cells and image transformation. I show that this software package can be further used to develop a generative adversarial neural network to virtually stain brightfield images of cells, replacing the traditional chemical staining for a downstream analysis of biological features. I then move on from applications in microscopy and image analysis to show the potential of deep learning in medical diagnosis. I show that dense neural networks perform better than simpler machine-learning algorithm and the clinical standard in the diagnosis of a genetic disease and in the prediction of short- and long-term morbidity in patients with congenital-heart-disease. At last, I have shown that a neural-network-powered strategy for testing and isolating individuals adapts to the parameters of a disease outbreak achieves an epidemic containment.

The interdisciplinary nature of the work in this thesis has allowed the application of new technologies developed in the field of physics to solve problems in the fields of biology and biomedicine, as well as overcoming barriers for the continued revolutionization of deep learning in microscopy.

Keywords: deep learning, neural networks, image analysis, microscopy, medical diagnosis

This thesis is based on the work contained in the following scientific papers:

Paper I: Digital video microscopy enhanced by deep learning

Saga Helgadottir, Aykut Argun and Giovanni Volpe

Optica **6**, 506-513 (2019)

Paper II: Quantitative Digital Microscopy with Deep Learning

Benjamin Midtvedt, **Saga Helgadottir**, Aykut Argun, Jesús Pineda, Daniel Midtvedt and Giovanni Volpe

Applied Physics Reviews **8**, 011310 (2021)

Paper III: Extracting quantitative biological information from brightfield cell images using deep learning

Saga Helgadottir*, Benjamin Midtvedt*, Jesús Pineda*, Alan Sabirsh, Caroline B. Adiels, Stefano Romeo, Daniel Midtvedt and Giovanni Volpe

arXiv preprint arXiv:2012.12986 (submitted 2020)

Paper IV: Virtual genetic diagnosis for familial hypercholesterolemia powered by machine learning

Ana Pina*, **Saga Helgadottir***, Rosellina Margherita Mancina, Chiara Pavanello, Carlo Pirazzi, Tiziana Montalcini, Roberto Henriques, Laura Calabresi, Olov Wiklund, M Paula Macedo, Luca Valenti, Giovanni Volpe and Stefano Romeo

European Journal of Preventive Cardiology, p.2047487319898951 (2020)

Paper V: The use of big data and deep learning to predict atrial fibrillation and mortality among patients with congenital heart disease

Kok Wai Giang*, **Saga Helgadottir***, Mikael Dellborg, Giovanni Volpe and Zacharias Mandalenakis

(submitted 2021)

Paper VI: Improving epidemic testing and containment strategies using machine learning

Laura Natali, **Saga Helgadottir**, Onofrio M. Marago and Giovanni Volpe

Machine Learning: Science and Technology (accepted 2021)

Reprints were made with permission from the publishers.

*Equal contributors

Contents

CHAPTER 1

Introduction

Let's start with the first day of my PhD. When I sat down with my supervisor Giovanni Volpe, he said that it is not possible to plan my studies from beginning to end, but that we would rather decide on a starting point and see how things would evolve from there. We did just that and I started my PhD as an experimentalist building a fluorescence microscope in the lab to study the interplay between swimming bacteria and their complex environments of passive Brownian microparticles. I even proceeded to extract the best swimmers from the bacterial strain and genetically engineer them to exhibit fluorescence. As you might notice, not exactly the topic of this thesis. Looking back, I am very glad indeed that we did not waste time trying to plan the coming years because I could not have imagined that I would end up with a PhD thesis about the application of deep learning in image analysis and medical diagnosis.

How did this topical shift happen? In order to study the interplay between the bacteria and the Brownian particles (Figure 1.2a), I had to track both types of objects. At that point I started having problems. Because of the low intensity of the fluorescence emission from the bacteria and the background light from the brightfield imaging of the Brownian particles, the microscopic images became noisy with an illumination gradient across images (Figure 1.2b) and changes in light intensity between frames based on how fluorescent the bacteria were in each frame. All this combined made it impossible to get a quality tracking using standard algorithmic approaches (Figure 1.2c). I struggled for a while before we decided to try something new. The hype of deep learning caught our attention and it didn't hurt to try that (Figure 1.2d). Spoiler alert: It worked, and solving previously unsolvable problems and improving performances compared to standard algorithmic methods with deep learning became the new passion of my PhD, to the point that today I don't even have access to the lab!

Let's first dig deeper into the topic of deep learning. Deep learning is a subcategory of machine learning and artificial intelligence, with artificial intelligence being an umbrella term for algorithms for task automations

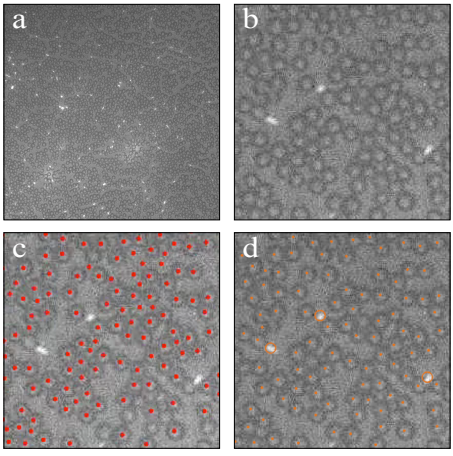

Figure 1.1: **The turning point of my PhD. a** An example of frame from my experiments with swimming fluorescence bacteria and passive Brownian particles. **b** Zooming in shows how noisy the image is. **c** Tracking with algorithmic methods results in multiple false positives in the top part and false negatives in the bottom part because of the inhomogeneous illumination. **d** Deep learning algorithms successfully track the Brownian particles and bacteria.

(Figure 1.2) [1]. The algorithms are either standard approaches that use explicit rules hardcoded by the user to perform the desired task, or machine-learning algorithms that autonomously learn from data to determine the rules for the task at hand. That is, instead of processing the data according to user-defined rules to find out the answer, the user inputs the data with the expected answers (supervised learning) to the machine and the machine is trained to learn the rules for this specific task. These rules can then be used to find the answers to new data. Therefore, a machine-learning model learns to transform its input data into more meaningful representations and the "deep" in deep learning means that successive layers of the model output increasingly meaningful representations of the input data, the number of these layers being called the depth of the model.

The most common deep-learning models are artificial neural networks. Artificial neural networks (ANNs) are inspired by the brain and it's ability to learn [2]. The layers in ANNs consist of interconnected artificial neurons that receive one or more inputs, sum them up and transform this sum by a non-linear activation function to produce an output. The connections between neurons in different layers have weights, which are (some of) the parameters adjusted in the training of the network. The training process is based on the *error backpropagation algorithm* [3], where the network first takes in input data and calculates a predicted output using the current weights of the

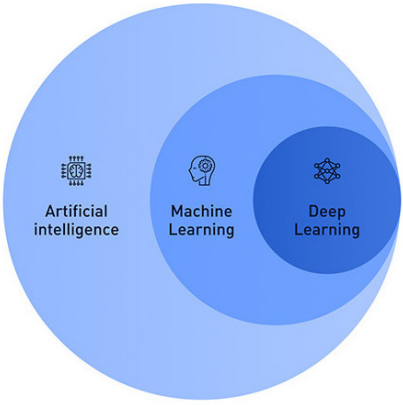

Figure 1.2: **Artificial Intelligence (AI) as an umbrella term.** AI simply means making computers act intelligently. Machine learning is a subset of AI, consisting of techniques that enable the computer to learn from data. Deep learning is then a subset of machine learning for solving more complex problems. Image by https://umbrellait.com/.

network. Next, the network compares the predicted output to the ground-truth answer and calculates an error based on the chosen *loss function*. The network then propagates the error backwards through the network and for each weight calculates if it should be increased or decreased in order to reduce the error. Finally, the network updates the weights in a way defined by the chosen *optimizer*. As the network receives additional training data, it gradually starts converging to an optimum weight configuration and the network is able to correctly map input data to their corresponding targets.

The idea of neural networks has been around since the 1950s, however the limiting factor was an efficient way to train larger networks. This changed partly in the 1980s when the error backpropagation algorithm was rediscover and a neural network called *LeNet* was successfully used to classify handwritten digits [4]. However it wasn't until early 2000s that the increase in available computational power and training data started the deep learning revolution. The breakthrough came with a neural network called *AlexNet* [5] placing top 5 in the well-known ImageNet challenge, where the task is to classify images into over 1000 different subcategories (http://image-net.org/ [6]). At the time, the ImageNet dataset contained over one million images and over 1000 subcategories and today has grown to have over 14 million images and over 20 thousand subcategories. The success of *AlexNet* resulted in the challenge being dominated by neural networks over other machine-learning techniques ever since and the image classification task considered a solved problem since 2017 with accuracy surpassing human abilities.

These first successful networks in computer vision were *convolutional neural networks* (CNNs) that take images as input and output a predicted class of the image [7]. CNNs are built on convolutional layers topped of with a few relatively small dense layers. Each convolutional layer consists of a series of 2D filters that scan an image to output a series of *feature maps*. The resulting feature maps are then downsampled before being fed to the next convolutional layer, where larger features can be detected. This is repeated depending on how deep the CNN is. The final dense layers integrate the information from the output feature maps before outputting the sought-after result, in this case the image category. In theory, *dense neural networks* (DNNs), consisting of a series of fully connected dense layers, could be used on their own to process images. However, because each neuron in one layer is connected to every neuron in the next layer, their size rapidly grows to computationally unmanageable levels. Therefore, they are often used in conjunction with convolutional layers or on their own for simpler problems represented by less complex data.

Going beyond image classification, a new kind of neural network called a *U-Net* was developed in 2015 for image segmentation [8]. The network gets its name from its U-shaped architecture: after a series of convolutional and downsampling layers that encode the information in the input image by reducing its dimensionality, a series of deconvolutional and upsampling layers follow in order to decode the image information. In addition, the decoding part concatenates information from the encoding part permitting the network to preserve spatial information to be able to reconstruct a transformed version of the input image. Using a U-Net in the framework of *Generative Adversarial Networks* (GANs) [9] allows it to be used to generate new data. A GAN combines two networks that compete with each other: A *generator* that receives images as input generates images in a different sought-after style, and a *discriminator* that tries to discriminate between real images and images generated by the generator. For image transformation tasks, the generator is typically a U-Net while the discriminator is a CNN classifying the images as real or fake.

In the recent years, deep learning has made great advances in solving various problems. In microscopy, deep learning has improved techniques for particle tracking [10–13] and characterization [14], depth-of-field extension [15, 16], image resolution [17, 18], image denoising [19, 20], and to translate the output of a certain optical device to that of another [21]. Apart from biological and medical image analysis [22, 23], where deep learning has been used for cell segmentation, classification and counting [8, 24–26], to classify pathological tissue samples [27–29] and to virtually stain cellular images [30–36], a vast amount of clinical, biochemical and administrative data is available to clinical specialist. Deep learning has utilized this data in healthcare for example for predictive modelling and aiding in disease diagnosis [37–41].

After this brief introduction into the history and research topics of neural networks concerning this thesis, I will present the challenges of using standard algorithmic methods for different problems and demonstrate how I solved them in my research by applying various types of neural network architectures. I found that deep-learning-powered solutions consistently have an increased performance compared to standard algorithmic methods and even simpler machine-learning methods. In particular, I show how deep learning makes novel tasks in image analysis possible and is useful in aiding in the diagnosis of diseases, the prediction of morbidity risks for patients, and in the construction of epidemic strategies. The increase in performance of the solutions presented in this thesis are especially important considering the relevance of the application fields to the real world, in particular the usefulness of the solutions in healthcare which has driven many of my projects that have been done in close collaborations with medical doctors specified in the field. In the following I will present for each study performed during my PhD: a short *motivation* and the *aim* of the study as well as the *main results* found.

1.1 Particle tracking with deep learning

Particle tracking has come a long way since Jean Perrin in 1910 manually tracked the positions of microscopic colloidal particles in a solution by projecting their image on a sheet of paper, thereby proving the physical existence of atoms [42]. Since the introduction of the technique generally referred to as "digital video microscopy" over 20 years ago [43], particle tracking has been dominated by algorithmic approaches. In digital video microscopy, a video of a particle is acquired and then the particle position in each frame is determined employing computer algorithms. Some of the most common standard algorithms are based on calculating the centroid of the particle in a black-and-white thresholded version of the image [43] or on calculating the radial symmetry center of the particle [44]. These methods can achieve subpixel resolution when the experimental conditions are ideal, with a spherically-symmetric particle that remains in the same focal plane during the experiment and with a constant homogeneous illumination. However, their performances decrease at low signal-to-noise ratios or under inhomogeneous illumination. This has led to the development of alternative deep-learning algorithms for particle tracking [10, 11].

The aim of this work was to develop a fully automated deep-learning technique that achieves subpixel resolution for a broad range of particle kinds, especially in poor, unsteady illumination conditions that result in noisy images. In **Paper I** [12], I report on a CNN network design trained with simulated images, that we call DeepTrack, that detects a single particle in microscopy images. We showed that DeepTrack outperforms standard methods when tested on simulated images with a range of signal-to-noise ratios and illumination gradients. We demonstrated this approach on

optically trapped particle under noisy and unsteady illumination conditions, where standard algorithmic approaches fail. We then proceeded to show how DeepTrack can track multiple colloidal particles as well as bacteria. In order to make DeepTrack readily available for other users, we provided a Python software package, which can be easily personalized and optimized for specific applications. These results are presented in section 2.1 and in **Paper I** [12].

1.2 Digital microscopy with deep learning

The success of DeepTrack and other deep-learning-based image analysis methods has also shed light on key limiting factors for the future development and deployment of deep-learning solutions to microscopy, that is the availability of high-quality training data. In many cases, training data has needed to be experimentally acquired and manually annotated for each specific application, limiting the quantity and quality of data available to train the network [45]. Synthetically generated data bypasses these issues because the ground truth can be known exactly, and the networks can be trained with parameters that exactly match each user's setup.

In **Paper II** [13], I report on a comprehensive software, DeepTrack 2.0 which greatly expands the functionalities of DeepTrack described in **Paper I** [12], to design, train and validate deep-learning solutions for digital microscopy. DeepTrack 2.0 goes beyond particle tracking towards a whole new range of quantitative microscopy applications, such as classification, segmentation, and cell counting. We briefly reviewed the main applications of deep learning to microscopy, with a special focus on image segmentation, image enhancement, and particle tracking, and the most frequently employed neural network architectures. Then, we demonstrated the versatility and power of deep learning and DeepTrack 2.0 by using it to tackle a variety of physical and biological quantitative digital microscopy challenges, from particle localization, tracking and characterization to cell counting and classification. For many of the tasks, we showed that DeepTrack 2.0 is capable of training neural networks using purely synthetic training data that are physically simulated using the nominal experimental settings. For tasks where it is infeasible to simulate the training set, DeepTrack 2.0 can augment experimentally-generated images on the fly to expand the available training set. We provided access to the software through three channels based on the user's level of expertise: from a graphical user interface, to scripts that can be adapted for specific applications, to a low-level set of abstract classes to implement new functionalities. In addition, we provided various tutorials to use the software at each level of complexity, including several video tutorials to guide the user through each step of a deep-learning analysis for microscopy. These results are also presented in section 2.2 and in **Paper II** [13].

1.3 Virtual staining with deep learning

With DeepTrack 2.0 we saw how the adoption of new deep-learning methods for the analysis of microscopy data is extremely promising. One of the areas of high interest today is using deep learning to create images of virtually-stained cell structures, thus bypassing the problems of conventional chemical staining. Traditionally, the cell structures of interest are chemically stained using fluorescence staining techniques and imaged with the appropriate light wavelength. Thanks to this, it is possible to highlight different cell structures in the same sample, given the appropriate combination of chemical dyes and light filters. This, however, is also one of the main drawbacks of the chemical staining: Only one cell structure can be stained with a dye emitting at a certain light wavelength at the same time as there is a limited number of light wavelengths and filters in the microscope, thus limiting the number of cell structures to be observed in the same sample. Other drawbacks of the chemical staining procedure are: First, adding a chemical dye to cells is an invasive and even toxic process [46, 47], second, phototoxicity and photobleaching can occur, resulting in a trade-off between data quality and time scales available for imaging of live cells, and third, chemical staining techniques are time-consuming and labor-intensive. Therefore, it would be optimal to be able to replace chemically-stained fluorescence images with other more easily acquirable images. In the recent years, virtually stained images have been created using various imaging modalities such as quantitative phase imaging [31, 48], autofluorescence imaging [32], holographic microscopy [49], and even with brightfield imaging [50–52].

In **Paper III** [30], I report on a deep-learning based approach to virtually stain brightfield images. In particular, we trained a conditional GAN (cGAN) using the DeepTrack 2.0 framework presented in **Paper II** [13] that receives as input a stack of brightfield images of human stem-cell-derived adipocytes and generates virtual fluorescence-stained images of their lipid droplets, cytoplasm, and nuclei. In order to demonstrate the quality of the virtually stained images beyond pixel error comparison, we used the images to extract a series of quantitative biologically-relevant measures in a downstream cell-profiling analysis [53]. With the lipid droplets having more prominence in the brightfield images than the cytoplasm, that, in turn, is more clearly visible than the nuclei, it is not surprising that the performance of the network follows the same trend. In addition, we showed that the cGAN is robust and fast-converging in terms of the extracted measures compared to a U-Net. In order to make this deep-learning-powered approach readily available for other users, we provided a Python software package, which can be easily personalized and optimized for specific virtual-staining and cell-profiling applications. These results are presented in section 2.3 and in **Paper III** [30].

1.4 Virtual genetic diagnosis with deep learning

Deep learning has not only been successful in image-analysis applications, it has also gained popularity in the field of medical diagnostics to process clinical and biochemical data [37–39, 41]. However, as deep-learning algorithms operate as "black boxes", their diagnoses cannot easily be interpreted or explained, which is an important aspect of the high-stake task being medical diagnosis [54]. In order to motivate the use of such black-box methods, there needs to be a clear advantage of using them over simpler machine-learning algorithms or other clinical methods.

The aim of the study in **Paper IV** [40] was to assess the use of machine-learning algorithms to implement a virtual genetic test for the genetic disease *familial hypercholesterolemia* (FH). FH is the most common genetic disorder of lipid metabolism, characterized by elevated LDL cholesterol levels resulting in premature cardiovascular diseases [55, 56]. The gold standard for FH diagnosis is genetic diagnosis, which is expensive, time-consuming, and only available at specialized lipid clinics and selected university hospitals [57, 58]. Clinical scores, like the Dutch Lipid Score [59, 60], are often employed as less expensive, but also less accurate, alternatives to genetic diagnosis [61]. We tested three machine-learning algorithms, namely, a classification tree (CT), a gradient boosting machine (GBM), and a dense neural network (DNN), and we showed that all three algorithms outperform the Dutch Lipid Score (the clinical standard) in detecting known FH genetic mutations. In addition, we showed that the more complex black-box methods GBM and DNN perform similarly between each other but had higher performances compared to the much simpler CT algorithm. These results are presented in section 2.4 and in **Paper IV** [40].

1.5 Prediction of morbidity with deep learning

Moving on from the genetic disease FH to *congenital heart disease* (CHD), the most common congenital malformation affecting almost 1% of all live-births worldwide [62, 63]. The severity of the condition varies depending on the congenital malformation specifics and the patients are often grouped into six groups based on the lesion severity [64, 65], with each group having its own probability of increased risk of cardiovascular diseases compared with a general population without CHD. The ability to predict morbidity such as atrial fibrillation (AF) and mortality can improve the use and timing of preventive medical treatments as well as the planning of lifetime management. However, few studies have reported on the long-term predictability of mortality and AF amongst patients with CHD.

In **Paper V**, I report on the prediction of short- and long-term mortality and AF from birth throughout the patients' lifetime using a DNN. We found that DNNs can be used to predict mortality and AF in a population of patients

with CHD in Sweden. When compared with a simpler logistic regression model, the DNN showed an overall higher predictive performance over time, most notably in mortality. When analysing the result for each lesion group, patients' birth decade, and patients that had undergone congenital cardiac interventions, we observed that the two methods have similar trends with the exception of the consistently higher performance of the DNN. These results are presented in section 2.5 and in **Paper V**.

1.6 Epidemic containment strategies with deep learning

Now, this wouldn't be a true "pandemic"-time thesis if it didn't include a Covid-19-related work. In the past year, we have seen the importance of implementing efficient strategies to contain a disease outbreak. Characteristics of a disease have to be taken into account in efforts of containment [66]. However, these characteristics are often difficult to measure or model precisely, especially during first outbreaks of novel diseases [67]. The most effective measure to limit the spread of an infection is in particular the isolation of potentially infected individuals. However, it is unreasonable to be able to test a whole population [68, 69]. Machine-learning algorithms, including neural networks, have, in the last years, been proposed for the management of infectious diseases [70–73].

In **Paper VI** [74], I report on a neural-network-informed strategy for the improvement of epidemic containment. We demonstrated how the DNN informs on which individuals should be tested and isolated for a disease outbreak modelled with the susceptible-infectious-recovered (SIR) model [75, 76]. The DNN manages to contain the outbreak more effectively than alternative standard contact-tracing strategies, while simultaneously and autonomously adapting to the specific characteristics of the outbreak. These results are presented in section 2.6 and in **Paper VI** [74].

Outline

This thesis is structured as followed:

Chapter 2 gives a summary of the research conducted during this PhD and specifies my contributions to each project.

Chapter 3 gives a general conclusion and an outlook into the future of this area of research.

Chapter 4 compiles all published articles.

CHAPTER 2

Research results

2.1 Particle tracking with deep learning

When we started the work for **Paper I** [12] in 2018, there were not many previous publications about deep-learning algorithms for the tracking of particles in microscopy images. Instead, the focus was on image classification and segmentation for object detection [77]. For precise particle localization, the most notable works were the use of CNNs, either trained on simulated fluorescence particles to output the probability of each pixel in a simulated or experimental image belonging to a particle or the background [11], or trained on synthetic holograms to localize holographic features in experimental holograms [10].

The problem that inspired the work in **Paper I** [12] had images with two kinds of particles, fluorescence bacteria (*B. subtilis*) and silica microspheres, which I wanted to track separately and ideally with the same technique and with minimum image preprocessing (Figure 1.1). In order to do so, we proposed a deep-learning approach based on a CNN with a DNN top, which we called DeepTrack (Figure 2.1a). Given an input image, DeepTrack returns the x and y coordinates of the particle, and the radial distance of the particle from the center of the image, r, which is used mainly to indicate whether there is no particle in the image. To have enough images with accurate ground-truth particle coordinates to train DeepTrack, we simulated particle images using Bessel functions of different orders. By setting the parameters of the image generation function, we were able to generate images representing fluorescence particles, biological vesicles and bacteria, and colloidal particles at different focal planes, with varying backgrounds, signal-to-noise ratios (SNRs) and illumination gradients (examples can be seen in the insets in Figure 2.1b).

First, we tested the performance of DeepTrack on simulated single particle images of various particle types with a range of SNR values and illumination gradients by comparing its localization accuracy with the standard centroid [43] and radial symmetry [44] algorithms (Figure 2.1b). We showed that

DeepTrack outperforms both standard algorithms over the whole range of illumination gradients and almost the whole range of SNRs, with the only exception of near-perfect images where the radial symmetry method achieves higher accuracy. However, neural networks can have a high variance as they are trained via a stochastic training algorithm, making them sensitive to the initial conditions of their weights and the specifics of the training data, which in turn leads to a different set of final weights each time they are trained and therefore different predictions. To reduce the variance of neural networks, multiple models are trained and their predictions combined, a technique called ensemble learning [78]. By training 100 neural networks with the DeepTrack architecture and the same data and average their prediction, we showed that with Deeptrack we are able to outperform both the standard algorithms over the whole range of images.

We next tested the performance of DeepTrack on experimental images of an optically trapped particle in ideal and poor illumination conditions, and again compared to the radial symmetry method (Figure 2.1c). We trained DeepTrack with simulated images similar to the experimental images, using the sum of Bessel functions of the first and second order with opposing intensities to represent the particle (a bright spot with a dark ring), and varying SNRs and illumination gradients for each image. As expected, both algorithms were able to track the particle in the ideal conditions. However, when the conditions become challenging with high level of noise and flickering of the illumination light, the radial symmetry method was not able to capture the particle position at all (capturing only white noise and oscillations of the illumination), while DeepTrack still managed to accurately track the particle position.

Now that we had demonstrated the performance of DeepTrack for single particle images, we moved on to multi-particle tracking. Since the architecture of DeepTrack has a fixed output of three values (x, y, and r coordinates for a single particle) we used a sliding window method where a box of a certain size (in relation to the particle diameter) is moved over the whole image with a certain step size. In each window, the neural network makes a prediction. In case there are more than one particles in the window, the network is trained to detect the most central particle. For an empty window where no particle is present, the network is trained to return a large radial distance (r). After DeepTrack has scanned over the whole image, the predictions from each window are further processed. First, coordinates from empty windows are discarded by their large radial distance parameter. Second, since the same particle can be detected in multiple windows (depending on window size and particle separation), all detections with an inter-distance smaller than a certain threshold are assigned to the same particle and their centroid is calculated to determine the particle position. Depending on the purpose of the tracking and the density of the particles in the image, the detection accuracy can be increased by decreasing the step size of the sliding window.

This, however, also becomes more computationally heavy.

At last, we were ready to tackle the problem that inspired the whole work, the tracking of noisy images of fluorescence bacteria and dense Brownian particles (Figure 2.1d). We trained two separate networks for each particle type. We simulated images of multiple particles of both kinds, using a second-order Bessel function to represent the Brownian particles (a dark ring) and a first-order elongated Bessel function to represent the bacteria (bright spots). For the network detecting Brownian particles, the most central particle is always set to be a Brownian particle, and the other way around for the network detecting bacteria. In this way, we showed that DeepTrack can be trained to selectively track either Brownian particles while ignoring the bacteria or bacteria while ignoring the Brownian particles.*

We further demonstrated the versatility of DeepTrack by tracking particles at different focal planes (Figure 2.1d). In this case, we trained DeepTrack with simulated images of multiple particles represented by combinations of Bessel functions of orders 1-4 (multiple dark rings) and successfully tracked an experimental video of polystyrene particles diffusing above the surface of a coverslip.

Finally, we benchmarked DeepTrack against a known objective comparison of particle tracking methods (all were based on standard algorithmic techniques) [79] (Figure 2.1e). We generated the test images representing fluorescent biological vesicles for different particle densities and SNRs in the same way as in the competitions. We trained DeepTrack with simulated images of multiple particles represented with a first-order Bessel function (bright spots) with varying SNRs. We showed that DeepTrack outperforms all other methods for all particle densities and SNRs when comparing the root-mean-square error (RMSE) for matching points in each frame, as was done in one part of the competition. We made DeepTrack readily available for other users by providing a Python software package, including Jupyter Notebooks for each example in the paper, which can be further personalized and optimized for specific applications [80].

The results of **Paper I** [12] clearly show the advances deep-learning methods have over standard tracking methods, and the advantages of being able to simulate accurate training data for diverse problems. DeepTrack proved to be a very accurate and efficient method for tracking single particles. However, sliding a window over an image to detect multiple particles becomes very time consuming for larger sets of data, as it requires the network to be called numerous times per frame. At the time of the writing of this thesis, **Paper I** [12] has been cited over 30 times, and a handful of new methods for multiple particle tracking have emerged. These include a CNN single-shot

*The work on the interplay of bacteria and Brownian particles is still in progress and a paper will sooner or later be published

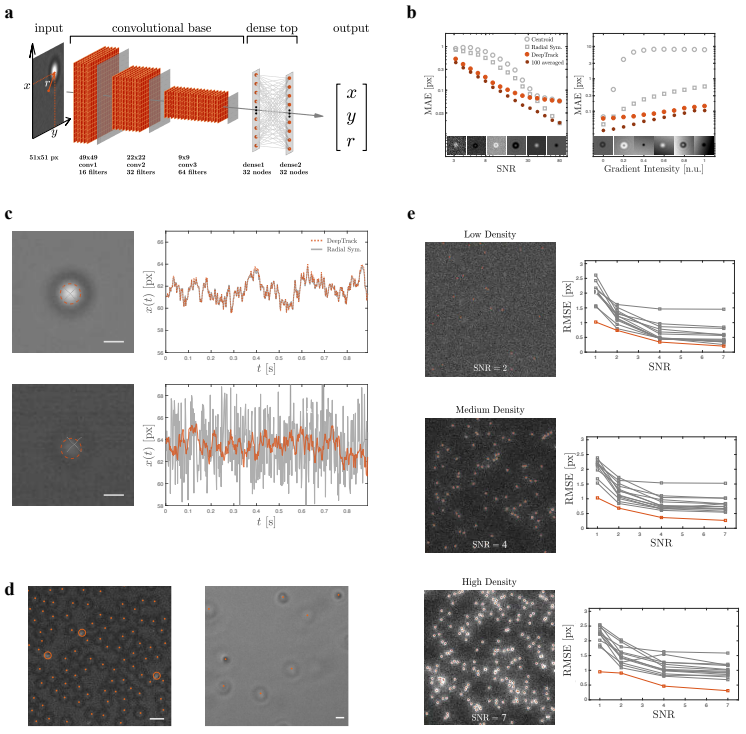

Figure 2.1: **DeepTrack neural-network architecture and performances.** **a** DeepTrack architecture consists of a convolutional base followed by a dense top to predict the values of the x, y, and r coordinates of the particle. **b** Mean absolute error of the position detection in simulated images as a function of signal-to-noise ratios and gradient intensity for DeepTrack (orange), standard algorithms (gray), and average of 100 DeepTrack networks (bordeaux). **c** DeepTrack (orange) and standard algorithm (gray) lead to the same results when tracking and analyzing the trajectory of an optically trapped particle under optimal illumination conditions but DeepTrack outperforms the standard algorithm in less-than-optimal illumination conditions. **d** DeepTrack can be trained to selectively track fluorescent bacteria or Brownian particles in poor illumination conditions as well as Brownian particles in different focal planes. **e** DeepTrack (orange) outperforms all other methods from an objective comparison on simulated data [79].

detector trained on synthetic images for the localization and classification of multiple microscopic objects in real time [81], a combination of a CNN and long short-term memory (LSTM) network trained on semi-synthetic images to detect overlapping traces particles in 3D [82], a multiple output CNN for the simultaneous detection characterization of nanoparticles [14, 83], and finally DeepTrack 2.0 (in **Paper II** [13]) which includes a U-Net trained on simulated images that transforms multiparticle images into binarized representations that can then easily be localized with standard methods [13]. Finally, **Paper I** [12] was highlighted in the end-of-year special issue of *Optics & Photonics News, "Optics in 2019"*, for being one of the emerging research the past year that communicated breakthroughs of particular interest to the broad optics community [84].

My contributions

Paper I [12] is a result of exceptional teamwork with my colleague Aykut Argun and supervisor Giovanni Volpe. I contributed to the conceptualization of the work, the design and development of the neural network, the simulation of the training images, acquisition of experimental data, analysis of the data, preparation of the figures and manuscript for publishing, and preparation of the free Python software package [80]. In particular, I conducted the simulations for all cases of the experimental particle images (in figures 2, 3 and 4) as well as the training of the network, analysis of its results, compilation of the corresponding Jupyter Notebooks (available on GitHub [80]), and figure preparation for the cases of multiple particles (figures 3 and 4). I drafted the original manuscript and was involved in the reviewing and editing until it was ready for publishing. In addition, I acquired the experimental data of colloidal particles and fluorescence bacteria used to demonstrate how DeepTrack can differentiate between two types of particles (in figure 4) using the homemade fluorescence microscope setup I had built and the bacteria I had engineered.

2.2 Quantitative digital microscopy with deep learning

Deep-learning approaches have greatly improved digital microscopy, because they potentially offer automatized, accurate, and fast image analysis. However, the need for the development of custom deep-learning solutions for each problem, like we've seen from the examples in the previous section (for **Paper I** [12]), introduces a steep learning curve and leaves the power of deep-learning for video microscopy underutilized. In **Paper II** [13] , we aimed to provide a solution to this issue in the form of a comprehensive software, called DeepTrack 2.0, which greatly expands the functionalities of the original DeepTrack from **Paper I** [12]. In DeepTrack 2.0, users can develop, train and validate neural networks for a broad range of tasks, using purely synthetic data generated within the software itself using physical

simulations or data augmentation on the fly to expand experimental datasets. In order to accommodate users with any level of expertise, we have made DeepTrack 2.0 available as a high-level graphical user interface and as scripts that can be adapted for specific applications.

In **Paper II** [13], we first provided a review of the history of quantitative analysis of microscopy images, from the manual tracking of Jean Perrin in 1910 [**Perrin1910MouvementMolecules**], to the automation of tracking in the 1980s [43, 87], and finally to image analysis with deep learning [8, 12]. Next, we gave an overview of the different deep-learning models that are most commonly employed in microscopy as well as reviewing the key applications of deep learning in microscopy, namely image segmentation, image enhancement, and particle tracking. We then proceeded to introduce DeepTrack 2.0. We described the different channels of access to the software, that is the graphical user interface, the Jupyter Notebooks, and the main components that the code for the software is built on and how these components interact. For the Jupyter Notebooks and the code components, we also provided several video tutorials [88]. Finally, we moved onto case studies that exemplify how DeepTrack 2.0 can be used for a broad range of microscopy applications (Figure 2.2). All these examples are available both as project files for DeepTrack 2.0 graphical user interface [89] and as Jupyter Notebooks [88], and they are complemented by video tutorials [88].

We started by showing that we can use DeepTrack 2.0 to employ a DNN to recognize hand-written digits of the MNIST dataset, which is a relatively simple yet a classical benchmark for machine learning [85]. We used the data augmentation of the software to train the network to achieve an accuracy which is comparable to the best performance using a DNN on the MNIST digit recognition task (Figure 2.2a). We then implemented in DeepTrack 2.0 the example of a single optically trapped particle in good and poor illumination conditions from **Paper I** [12]. The only difference was that that DeepTrack 2.0 allows the generation of the training data using the properties of the microscope used to capture the data and the properties of the microscopic particle such that the synthetic data closely matches the experimental image (Figure 2.2b). In the next example, we used DeepTrack 2.0 to develop a model based on a combination of a CNN and a DNN trained on synthetic images (based on the experimental conditions) to quantify the radius and refractive index of particles based on their experimental complex-valued scattering patterns from an off-axis holographic microscope [14]. We showed that we are able to clearly distinguish two particle populations, closely matching the modal characteristics of the particles (Figure 2.2c).

After these initial examples for analysing single particles, we moved on to more complex tasks involving the analysis of multiple particles. We began by demonstrating the tracking of multiple particles in 2D (Figure 2.2d). We trained a U-Net with synthetic data simulating the appearance of quantum

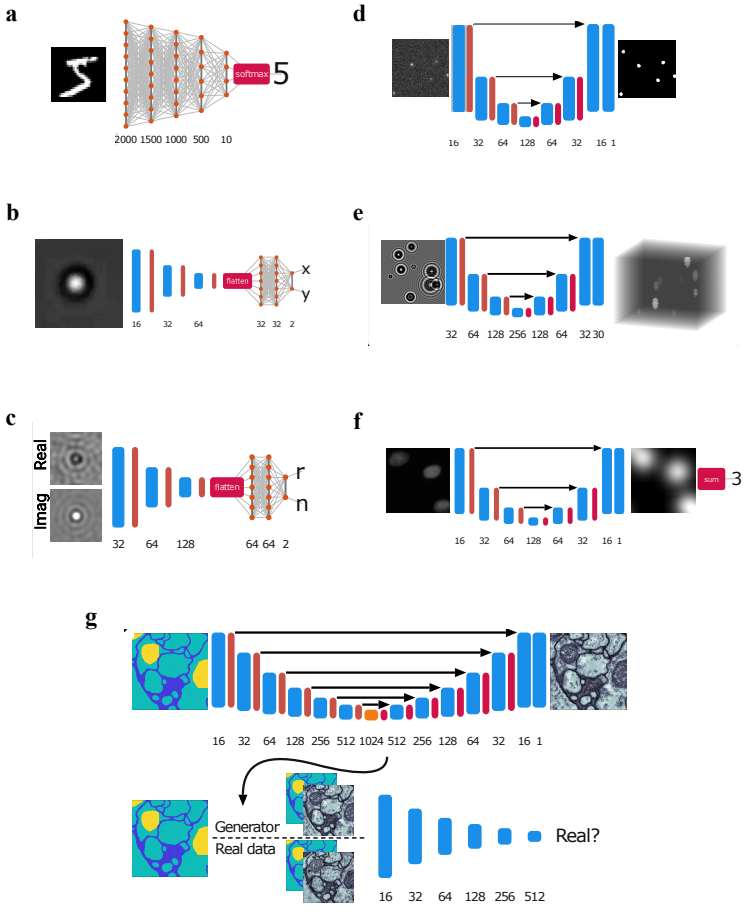

Figure 2.2: **Case studies that exemplify how DeepTrack 2.0 can be used for a broad range of microscopy applications.** **a** A dense neural network (DNN) to classify handwritten digits from the MNIST dataset [85]. **b** A convolutional neural network (CNN) to track single particles in brightfield images. **c** A convolutional neural network (CNN) to measure the radius and refractive index of single holographic nanoparticles. **d** A U-Net to detect quantum dots in fluorescence images. **e** A U-Net to track holographic spherical particles in 3D. **f** A U-Net to count cells in a fluorescence image. **g** A generative adversarial neural network (GAN) to create cell images from a semantic mask from the ssTEM dataset [86].

dots[†] to transform the input into a binarized representation of white circles on a black background that can then easily be tracked using standard algorithmic methods. Qualitatively, as we did not have a ground truth for this problem, the model detects all obvious particles, as well as a few that are hard to verify as real or false observations. We then showed that 2D multi-particle analysis can be extended to 3D in DeepTrack 2.0 (Figure 2.2e). Similarly, we used a U-Net to represent each particle as a white sphere in a black volume, as well as outputting the out-of-plane position of the particle. Training the network using synthetic data representing holographic nanoparticles resulted in predictions of the 3D locations of the particles overlapping almost exactly with the ground truth experimental data using off-axis holographic microscope.

Finally, we expanded DeepTrack 2.0 outside of particle analysis to the analysis of biological cells. We again used a U-Net, but now representing cells by a Gaussian distribution whose intensity values integrate to one, making the integral of the output intensity correspond to the number of cells in the image (Figure 2.2f). The model is trained using synthetic images of fluorescence cell-like objects and successfully counts the number of bone tissue cells in fluorescence images within just a few percent. As a final example, we demonstrated how DeepTrack 2.0 can be used to generate data (Figure 2.2g). We employed a GAN to create images of the *drosophila melanogaster* third instar larva ventral nerve cord from a semantic representation of background, membrane, and mitochondria from the anisotropic ssTEM dataset [86]. Since the training data consists of experimental data, DeepTrack 2.0 was used to preprocess and augment the training images. The resulting model was able to create new images from masks it has never seen before. The generated images are qualitatively similar to the experimental images, although not identical in terms of texture and appearance, since the masks only contain spatial information about the cells' structures.

In **Paper II** [13], we have shown that DeepTrack 2.0 has the potential to be an all-in-one framework for deep learning in microscopy. The image generation pipeline included in DeepTrack 2.0 allows for physically accurate synthetic training images based on parameters that exactly match each user's real experimental conditions, thus bypassing the issues of manually annotated experimental data alongside its limits of human-level accuracy and biases. For most applications, DeepTrack 2.0 already includes all necessary components for simulation of training images and development of neural network models. However, for the more advanced users, DeepTrack 2.0 is built to be easily extendable and, in fact, as we envision DeepTrack 2.0 as a open-source project, we hope and expect users to expand its functionalities according to their needs. We are now planning to provide tools to integrate

[†]Data kindly provided by Carlo Manzo

DeepTrack 2.0 with the popular (especially amongst biologists and medical researchers) image processing package Fiji [90], making image analysis with deep learning readily available for people in the fields of biology and medicine. Since its very recent publication, we have already assisted other researchers in using DeepTrack 2.0 in their projects, including 3D tracking and classification of holographic micro planktons, aberration correction in light-sheet microscopy and 3D super-resolution fluorescence microscopy from 1D time responses. We have also published a summary of the work in Swedish in *Fysikaktuellt*, the magazine of the Swedish Physical Society [91].

My contributions

Paper II [13] is a work of art developed mainly by my colleague Benjamin Midtvedt that I am grateful I got to be a part of. In this work, I wrote the draft of the review of the history of quantitative microscopy and particle tracking for the manuscript's introduction as well as contributed to the reviewing and editing of the whole manuscript for publication. I contributed to the development of the software with a series of testing and feedback as well as making the video tutorials for two of the examples presented [88]. In addition, I proposed the description of the interaction between the main component objects DeepTrack 2.0 solutions depend on (part III-C and figure 6). Finally, the case study for particle localization is from DeepTrack in **Paper I** (part IV-B and figure 8)[12].

2.3 Virtual staining with deep learning

As we have seen in **Paper II** [13], deep learning, in particular GANs, can be used to generate never-before-seen images. In microscopy, GANs have been used to improve the resolution of fluorescence images [18], in image denoising [20, 34], and to create images of virtually-stained cell structures from images acquired with various imaging modalities. Examples of virtual stainings include histologically stained brightfield images generated from quantitative phase image [31], autofluorescence images [32, 48] and brightfield images [51], and fluorescently stained images generated from holographic microscopy [49] as well as brightfield images [50]. Using deep learning to generate virtually stained images bypasses the significant drawbacks of chemical staining: First, the need for a fluorescence microscope with the appropriate filters, second, that only one dye can be imaged at a specific wavelength, third, that chemical dyes can be toxic to the cells (we have seen preliminary evidence of this in a follow-up work not included in this thesis), fourth, that phototoxicity and photobleaching prohibit longer time scales for live-cell imaging, and fifth, that chemical staining techniques are expensive, time-consuming and labor-intensive.

In **Paper III** [30], we proposed a deep-learning-based approach to virtually stain brightfield cell images demonstrating that we could extract quantitative

biological information from the virtually stained images, going beyond only using mean absolute error (MAE) for the quantitative comparison with the ground-truth chemically-stained images (Figure 2.3a shows an overview of the study). In particular, we developed a conditional GAN (cGAN) using the DeepTrack 2.0 framework from **Paper II** [13] to receive a stack of brightfield images of an adipocyte cell culture at different z-positions and generate virtually-stained fluorescence images of the cells' lipid droplets, cytoplasm, and nuclei. The *conditional* aspect of the cGAN refers to the fact that the task of the discriminator is conditioned on the brightfield images, i.e., instead of answering "is this a real staining?", the discriminator answers "is this a real staining *for this stack of brightfield images*?"

The cell culture was imaged at three magnifications (20×, 40× and 60×) and we trained one cGAN for each of the datasets. Qualitatively, the networks were able to generate realistic virtually-stained fluorescence images of lipid droplets, cytoplasm and nuclei for all magnifications (Figure 2.3 shows an example for 60× magnification). The lipid droplets were virtually stained with great detail, as would be expected since lipids have a higher refractive index than most other intracellular objects [92], making them clearly visible in the brightfield images. The cytoplasm also has quite good contrast in the brightfield images, resulting in high-quality virtual staining. The cGAN also managed to identify the nuclei, even though it seems to extract information about their shape based on the surrounding cell structures. This is evident from the fact that the cGAN often missed nuclei that are not surrounded by lipids and is not able to resolve the details of their internal structure. This is not surprising since the nuclei have a very similar refractive index to the surrounding cytoplasm [93] and sometimes seemed partly hidden behind the lipid droplets. For the quantitative analysis, we compared both the normalized mean absolute error (nMAE), structural similarity index measure (SSIM), and the peak signal-to-noise ratio (PSNR), and the extracted biologically-relevant features from a downstream cell-profiling analysis, between the target fluorescence images and the virtually-stained fluorescence images. We used a custom-made feature-extraction pipeline (available in [94]) in the open-source image analysis software CellProfiler (https://cellprofiler.org, version 4.07 [53]) to calculate the number of cell structures in each image, their mean area in pixels, their integrated intensity, their mean intensity, and the standard deviation of their mean intensity. We have demonstrated that there is a high correlation between all metrics obtained with the target fluorescence images and the virtually-stained fluorescence images, indicating that any deviation between the images is systematic and consistent, which is highly relevant for biological experiments where the comparison between different samples is often more important than absolute values. We also showed that the cGAN is robust and fast-converging in terms of the extracted measures compared to a U-Net previously used for virtual staining [50], with a marginal increase in quantitative performance after only a short training.

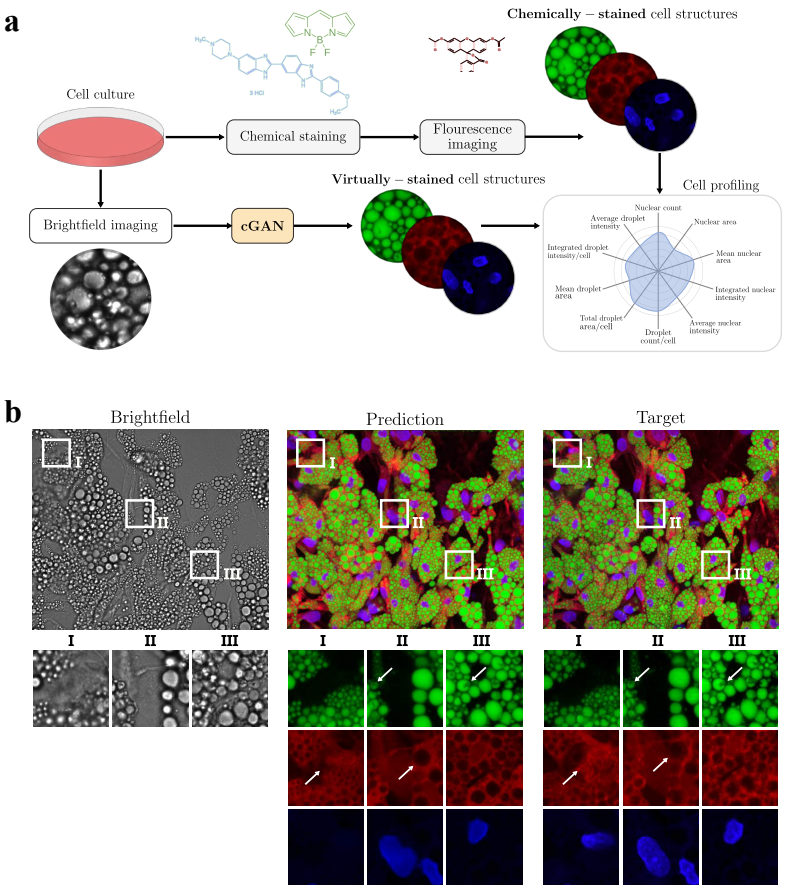

Figure 2.3: **a From cell cultures to quantitative biological information.** The generative adversarial neural network (cGAN) replaces the chemical-staining and fluorescence microscopy (multiple channels) by using brightfield images to generate virtual fluorescence-stained images. **b** Visualization of virtually-stained fluorescence images. A brightfield image and corresponding merged virtually-stained and chemically-stained fluorescence images for lipid droplets, cytoplasm and nuclei and their individual enlarged crops (green, red and blue, respectively). The chemical staining of lipid droplets and cytoplasm is accurately predicted by the virtual staining, even reproducing some detailed inner structures (indicated by the arrows). The virtually-stained nuclei deviate more prominently from the chemically-stained ones, especially in the details of both their shape and texture.

Virtual staining techniques have the ability to be a more robust than the conventional chemical staining techniques. They are less labor-intensive and independent of carefully optimized staining procedures, making possible the comparison of stained images across experiments and labs. As always, we made this deep-learning-powered approach readily available for other users by providing a Python software package, which can be easily personalized and optimized for specific virtual-staining and cell-profiling applications [94]. We are now using the same network for two different datasets in follow-up works that are not included in this thesis (cell viability in human endothelial cells and fat reduction in human hepatocytes) and we have helped researchers outside our group getting it working on their dataset.

My contributions

The work for **Paper III** [30] started with *The Adipocyte Cell Imaging Challenge*, a two week intense challenge organized by AI Sweden and AstraZeneca, and was ready for submission in less than two months. **Paper III** [30] is thus another great example of teamwork where my colleagues Jesús Pineda and Benjamin Midtvedt and I worked day and night to be able to submit the manuscript before Christmas (making it on Arxiv December 25, 2020), hence the shared first authorship. The idea for this work was inspired by the challenge and the data was provided by one of the challenge organiser and our collaborator Alan Sabirsh from AstraZeneca. I contributed to the conceptualization of the solution we developed for the challenge. The neural network we used is based on DeepTrack 2.0 from **Paper II** [13] and was optimized for this dataset by Benjamin and Jesús, who were also in charge of the training of the network. I was in charge of the evaluation and analysis of the network output that was based on the comparison to the ground truth images, using both the pixel measures and the downstream cell-profiling analysis. I contributed to the preparation of the manuscript and the figures (especially figures 2, 3 and 4) and the corresponding text in the manuscript. The biological relevance of the work was provided by our close collaborators Caroline B. Adiels from our neighboring research group at the department of physics and Stefano Romeo from Sahlgrenska Academy at the University of Gothenburg.

2.4 Virtual genetic diagnosis with deep learning

Even though deep learning is more flexible than other machine-learning approaches, deep neural networks generally require larger sets of training data, as a consequence of their depth and large number of trainable parameters. Given the increase in available data in biomedical fields, it is not surprising that more studies using deep learning for medical diagnosis are emerging [37]. One of the main limitations for the adaptation of deep-learning solutions in biomedicine is the need for model interpretability, because understanding the model's predictions is often just as important as

achieving accurate results. In a high-stakes task such as medical diagnosis, simpler transparent machine-learning approach could thus be preferred over a more complex deep-learning algorithm [54]. When it comes to *familial hypercholesterolemia* (FH), machine learning has been used to screen a general population using number of features from electronic health records [95], and in order to aid physicians in selecting people that have increased LDL cholesterol from a general population for genetic testing [96].

In **Paper IV** [40], we used three machine-learning algorithms (CT, GBM and DNN) to predict the presence of FH-causative genetic mutations in patients from lipid clinics in Gothenburg, Sweden, and in Milan, Italy. We trained all the algorithms using the subjects' LDL and HDL cholesterol levels, triglyceride levels, and age, which are all clinically relevant traits measured in every lipid clinic, as input variables. 70% of the Gothenburg dataset was used for training and the algorithms were tested internally on the remaining 30% of the Gothenburg dataset and externally on the Milan dataset. As machine-learning algorithms are prone to variance in their training [78] and both the Gothenburg and Milan datasets were relatively small (N=248 and N=364, respectively), in order to make the results more reliable, we trained each algorithm 100 times (with random splits of the Gothenburg dataset), resulting in 100 classifiers for each machine-learning algorithm. We evaluated the algorithms' performances by calculating their area under the receiver operating characteristic (AUROC) curves and showed that all machine-learning algorithms performed better than the Dutch Lipid Score, which is the commonly employed clinical alternative to the gold standard genetic testing, taking into account patient's clinical and family history, their LDL cholesterol, and physical examination. This is interesting considering that while FH is a genetic disease, the machine learning only use personal information, not depending on family history awareness. Furthermore, we showed that there is a trade-off between having a transparent and interpretable algorithm and higher performance as the black-box models GBM and DNN performed better than the simpler CT. An overview of the study is shown in Figure 2.4.

The main limitation of the work in **Paper IV** [40] is the low number of subjects in the datasets. After the publication, we have gotten access to additional data from the lipid clinic in Milan and, with some tweaks to the DNN, I have managed to further increase its performance when training using the Gothenburg dataset and testing externally on the Milan dataset and vise versa. We also speculate that the performances of the scalable DNN and GBM would increase with the addition of other clinically relevant biochemical features as input variables. Finally, we have found that there is a great interest among specialists in an alternative tool for the aid of FH diagnosis. I have therefore built a prototype application using the DNN algorithm developed in **Paper IV** [40]. By determining certain cut-off points with a specific sensitivity and specificity, the application can be used to

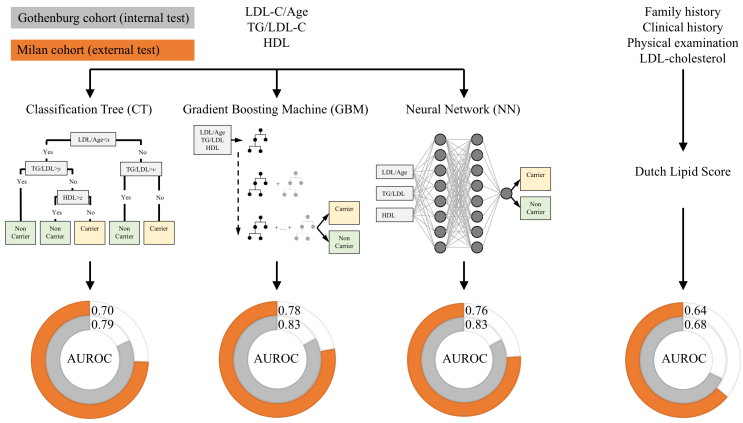

Figure 2.4: **Virtual genetic diagnosis.** All three machine-learning algorithms (classification tree (CT), gradient boosting machine (GBM), and neural network (NN)) performed better than the clinical Dutch Lipid Score in predicting carriers of FH-causative mutations in two independent FH cohorts (from Gothenburg and Milan)

decide if a genetic test for determining if the patient has FH is necessary. The application can with certainty predict the patients that definitely have or do not have FH, thus reducing the amount of genetic tests performed. At the time of the writing of this thesis, we are preparing a trial to use this application in Gothenburg. We have also published a summary of the work in Swedish in *Fysikaktuellt*, the magazine of the Swedish Physical Society [97].

My contributions

Paper IV [40] is the result of interdisciplinary and international collaboration. I developed the neural network and analysed its results. I drafted the manuscript and contributed to the preparation of the figures and the final manuscript. The two other machine-learning algorithms were developed by Ana Pina from Nova University of Lisbon. Before I became a part of the project, it had already been decided that Ana would have first authorship, however, as I came in and continued to drive the project we agreed to share the first authorship. The data was gathered by Rosellina M. Mancina from Sahlgrenska Academy at the University of Gothenburg, Carlo Pirazzi from Sahlgrenska University Hospital, and Chiara Pavanello from the University of Milan.

2.5 Prediction of morbidity with deep learning

Managing diseases after they have been diagnosed is just as important as the diagnosis itself. In disease diagnosis and prognosis, machine learning and deep learning has been used to analyse clinical and biochemical data [37]. *Congenital heart disease* (CHD) is the most common congenital malformation, affecting almost 1% of all live-births and often leading to lifelong medical conditions [62, 63]. The severity of CHD varies depending on the congenital malfunction, with patients often being grouped into six lesion groups based on the lesion severity, and along with the varying severity comes the increased risk of cardiovascular diseases and reduced life expectancy [98–100]. Prediction of morbidity (such as mortality and atrial fibrillation (AF)) is important as it can influence how and when to use preventive medical treatments. In a previous work, multiple deep learning algorithms were used to analyse complex data from an adult population including clinical and demographic data, ECG parameters, exercise, and selected laboratory markers to categorize diagnostic group, disease complexity, estimate its prognosis and guide the patient therapy [101]. However, such data may not be routinely available for the regular clinician.

In **Paper V**, we proposed a DNN (Figure 2.5a), trained on few easily obtainable variables from administrative data available in medical records, to predict short- and long-term (1-, 3-, 5-, 10-, 20-, and 30-year) mortality and AF from birth in a total of 71,941 CHD patients born between 1970 and 2017 from a nationwide population obtained from the Swedish National Patient Register. We further used a logistic regression (LR) based on the same data as a baseline comparison. The input variables used to predict mortality of CHD patients included the age of onset of the common comorbidities AF, heart failure, hypertension, diabetes, myocardial infarction, as well as the age of congenital cardiac intervention, the patients' age, decade of birth, sex, and lesion group. To predict the development of AF, we used the same input variables only excluding information about AF. To account for patient development, a cross-section over each patient's lifetime (until AF event for the case of predicting AF) was constructed, expanding the dataset to 1,214,121 data points for the prediction of mortality and 1,205,180 data points for the prediction of AF. For each case of 1-, 3-, 5-, 10-, 20-, and 30-year predictions for mortality on one hand and AF on the other, 10 DNNs were trained with random splitting of the datasets into training (70%) and testing (30%) sets. The performance of each of the DNNs and their average was evaluated using AUROC curves similarly to **Paper IV** [40]. Overall, the DNNs were successful in predicting the mortality and AF among CHD patients with an average performance higher than LR from the first to the last year (examples are shown in Figure 2.5b). We also broke down the performance dependencies on the patients' lesion group, birth decade and surgical intervention, and we showed that even though the average performance of the DNNs is stable and independent of the specific input

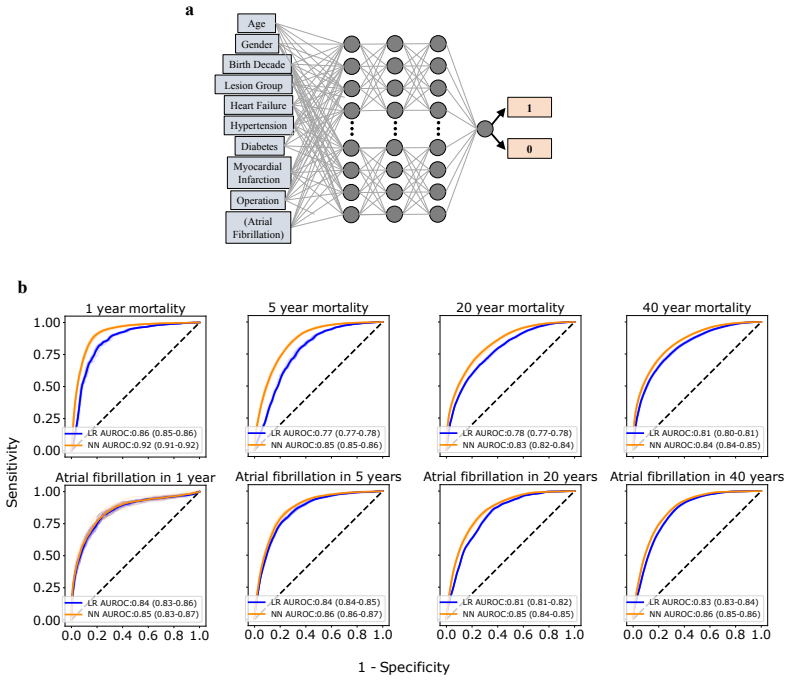

Figure 2.5: **Prediction of atrial fibrillation and mortality among patients with congenital heart disease using.** **a** The neural network uses easily attainable patient variables to predict **b** the short- and long-term mortality and atrial fibrillation more accurately than a simpler logistic regression model.

variables there is a higher variance in the models' output for more complex lesion groups especially. In comparison, the average performance of the LR models is lower with a higher internal variance in general.

In contrast to **Paper IV** [40], here we had a large nationwide dataset, including also patient development from birth which is especially important as the highest relative mortality occurs during the first five years of a patient's lifetime [102]. As in **Paper IV** [40], we also supported the predictions of a black-box model with a more simple, albeit less stable, machine-learning model. We have again prioritised using few, easily-attainable input variables, however, it could also be promising to combine the administrative data used here with clinical and socio-economical data, to further increase the usefulness of deep learning in this complex, heterogeneous, and vulnerable patient group.

My contributions

The work for **Paper V** was done in collaboration with Kok Wai Giang, Mikael Dellborg and Zacharias Mandalenakis from Sahlgrenska Academy at the University of Gothenburg and Sahlgrenska University Hospital (Östra sjukhuset). I preprocessed and constructed a cross-section of the data, developed the neural network and logistic regression used to analyse the data, prepared all the figures, wrote the methodology of the manuscript, and contributed to reviewing and editing of the manuscript. My collaborators gathered the data, put the results in medical context, and contributed to preparing the manuscript, resulting in a shared first authorship.

2.6 Epidemic containment strategies with deep learning

In addition to aiding in disease diagnosis and prognosis, deep-learning approaches can be used for infectious disease management [70, 103, 104]. Containment of disease outbreaks are of specific interests in the current times and neural networks have already been suggested as potential candidates for the detection and prediction of Covid-19 [71–73, 105]. Different containment strategies taking different constrains into account have been employed around the world in the past year. As is is not feasible to test all individuals of a population and only isolate the infectious ones [69, 106, 107], measures, such as partial or complete lockdown of a society, affecting also healthy individuals are taken. In order to minimize the societal and economic costs of such measures, it is important to identify an optimized test strategy.

In **Paper VI** [74], we proposed a neural-network-powered strategy based on DNNs for testing and isolating individuals that adapts to the parameters of a disease outbreak. We first modeled an epidemic outbreak using an agent-based SIR model (Figure 2.6a) [108, 109], where individuals move as random walkers on a square lattice. Individuals were characterized by their "temperature" (Figure 2.6b) and at the beginning of the simulation a number of individuals were randomly made infectious (I) and the rest are susceptible (S). As the disease outbreak evolves, susceptible individuals that get into contact with infectious ones can get infected, and, with time, infected individuals recover (R). We then demonstrated that our neural-network-informed strategy, taking in information about individuals' number of infectious and total contacts and the number of individuals that have tested positive within a certain radius, achieves an epidemic containment similar to the unrealistic *total lockdown* policy, while performing the same number of tests, only isolating 25% of the population and with a much lower number of total infected individuals compared to the standard *contact tracing* strategy [106, 107, 110, 111] (6-14% to 30-89%, respectively (Figure 2.6c). The same was true when we considered the case when immunity against the disease is not permanent, that is when recovered individuals can become susceptible again (SIRS model) [112–114]. In addition, we showed that the

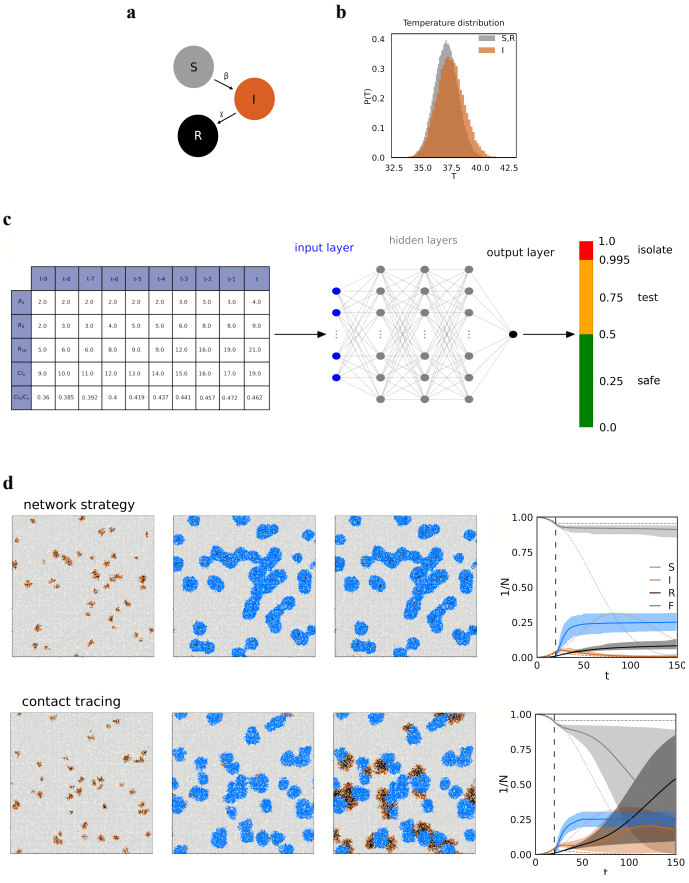

Figure 2.6: **SIR model and containment strategies. a** Each individual is either susceptible (S, grey), infectious (I, orange), or recovered (R, black). **b** Individuals are characterized by their "temperature". **c** The neural network's input consists of contact-tracing information for a given individual n for the last 10 time steps. The network outputs a value p between 0 (healthy) and 1 (infectious), representing the risk of being infectious at the current time step. **d** Disease evolution when testing and isolation strategy is determined based on the output from a neural network compared to standard contact-tracing strategy is shown as snapshots at time steps. The two limiting cases of free evolution (dotted orange line) and full lockdown (dashed orange line) are shown for comparison.

neural network automatically and dynamically adapts itself to the underlying characteristics of the outbreak as well as its evolution patterns by taking into account the effects of the containment measures that have been taken. The network could thus be used on more complex epidemiological models including for example the disease incubation time [67], delays in the testing process [107], and different individual movement patterns [115]. Additional input variables such as demographic information, such as age, employment and pre-existing conditions could also be used to potentially increase the network performance.

My contributions

Paper VI [74] is a beautiful work done mostly by my colleague Laura Natali. In this work I used the experience I had gained to assist Laura in the development of the neural network and the analysis of its results. I also contributed to the reviewing and editing of the manuscript.

CHAPTER 3

Conclusions and outlook

The idea of deep learning has been around since the 1950s [1]. However, until recently, it was limited by available computational power and amount of training data. The deep-learning revolution started with neural networks dominating in image classification challenges [6], and with the development of the U-net [8], introducing a wave of novel methods for image analysis and image transformation, outperforming standard methods in all disciplines.

In the beginning of my studies, I stumbled upon a problem when analyzing experimental microscopy data that I solved by developing a convolutional neural network (CNN) trained with simulated particle images to track different kinds of experimental single particle images (DeepTrack in **Paper I** [12]). This shifted the focus of my research and the work in **Paper I** [12] inspired the development of an all-in-one software to design, train and validate deep-learning solutions for digital microscopy (DeepTrack 2.0 in **Paper II** [13]). One of these solutions is a virtual fluorescence staining of brightfield images using a conditional generative adversarial network (cGAN) that can replace a chemical staining of intracellular structures of human adipocyte cells, where the cGAN is very robust and fast-converging in terms of biologically-relevant features extracted from the stained images (**Paper III** [30]). Besides deep-learning applications in microscopy and image analysis, it also has potential in medical diagnosis. This is evident in dense neural networks (DNNs) performing better than simpler machine-learning algorithm and the clinical standard in the diagnosis of a genetic disease (**Paper IV** [40]) and in the prediction of short- and long-term morbidity in patients with congenital-heart-disease (**Paper V**). At last, a neural-network-powered strategy for testing and isolating individuals is able to adapt to the parameters of a disease outbreak achieving an epidemic containment similar to the unrealistic *total lockdown policy* (**Paper VI** [74]).

I have shown that a data-driven neural-network approach, that we call DeepTrack, enhances digital video microscopy going beyond the state of the art available through standard algorithmic approaches to particle

tracking (**Paper I** [12]). DeepTrack can be trained with simulated images closely resembling a variety of experimentally relevant images and outperforms traditional algorithms, especially when image conditions become non-ideal due to low or non-uniform illumination, allowing the tracking of particles from videos acquired in conditions currently not trackable with alternative methods. I have then shown that DeepTrack can be expanded to a comprehensive software environment for the development of neural-network models for quantitative digital microscopy, from the generation of training datasets to the deployment of personalized deep-learning solutions (DeepTrack 2.0 in **Paper II**). With DeepTrack 2.0 it is possible to train neural networks that perform a broad range of tasks, from tracking and characterization of particles in 2D and 3D to cell segmentation, characterization and counting, either using purely simulated training data or by augmenting images on the fly to expand the available training set.

I have also shown that a cGAN developed with DeepTrack 2.0 can virtually stain brightfield images of human adipocytes to generate fluorescence images of the cells' lipid droplets, cytoplasm and nuclei, that can subsequently be used for quantitative analysis of the intracellular structures in terms of their size, morphology and content (**Paper III** [30]). The adversarial aspect of the cGAN makes it fast convergent compared to using a U-Net only minimizing the pixel loss. The resulting excellent style transfer and the conditionality of the cGAN becomes evident in the accurate extraction of biologically-relevant features from the reconstructed images. The proposed approach is not limited to the imaging modality, type of staining, the cellular culture, or the structures quantified in **Paper III** [30], but can be applied to virtually stain and quantify any cellular and intracellular objects with unique optical characteristics. In addition, using virtual staining liberates the fluorescence channels in the microscope so that additional information, that perhaps is not optically visible, can be obtained using chemical staining.

An important aspect of **Papers I-III** [12, 13, 30] is that the corresponding code is available as a open-source Python software package on Github. There the hope is that other researchers personalize and optimize the code for their specific applications. It is especially encouraged that people contribute objects and models in their area of expertise in order to continuously build DeepTrack 2.0 as an open-source software package to revolutionize microscopy with deep learning. This along with DeepTrack's graphical user interface and addition to ImageJ will hopefully allow users from all fields and minimal programming experience to take advantage of deep learning in their research. In my experience, I have seen that the availability of quality representative data (experimental or simulated) is the single most important factor for successful deep-learning solutions. Increased availability of physical simulations of in-sample structures (especially biological specimens) and optical setups plays a crucial role for the expansion of deep learning in microscopy. In **Papers I-II** [12, 13] I had the luxury that the experimental

data to be analysed were easily simulated, creating enough training data with accurate ground truth information. The dataset for the virtual staining in **Paper III** [30] was, while complex in its nature, also of high quality. However, when applying the cGAN on other datasets, I have seen the importance of the number of uncorrelated images in the dataset, the number of cells in each image, and the consistency of the ground truth chemical staining.

Machine learning and deep learning can also be used to aid in medical diagnosis. I have shown that machine-learning algorithms (namely, a classification tree (CT), a gradient boosting machine (GBM) and a dense neural network (DNN)), using only a few clinically relevant parameters, outperform the clinical standard in detecting carriers of gene mutations in patients from two independent familial hypercholesterolemia (FH) cohorts from Gothenburg and Milan (**Paper IV** [40]). The more complex models, DNN and GBM, performed better than the simpler CT. This is an especially important insight when it comes to medical diagnosis, creating a trade-off between higher performance of so-called "black-box" models and interpretability of transparent models. The machine-learning algorithms only make use of personal information (age and the widely assessed lipoprotein profile), not depending on family history and physical examination like in the clinical score. It is highly likely that the performance of the algorithms would increase with a higher number of patients in the training cohort and using additional relevant biochemical features. These features and numerous patients were not included in the datasets in **Paper IV** [40] because of the problem of missing data, which could be improved with new and reliable ways of training neural networks in the presence of missing data.

I have also shown that deep learning, in particular a DNN can be used to predict short- and long-term mortality and atrial fibrillation in people with congenital heart disease (CHD) on a nationwide scale using data that are easily obtainable by clinicians, outperforming in most cases the more traditional logistic regression (**Paper V**). A reliable prediction of morbidity is important to focus preventive action and treatments for CHD patients, whether it is to not intervene too early or too late. While administrative data like the data used in **Paper V** are easily attainable, a combination of administrative, clinical, and even socio-economical data could be promising for future use in DNNs in this complex, heterogeneous, and vulnerable patient group. Finally, I have shown that a neural-network-informed strategy is able to improve the containment of an epidemic (**Paper VI** [74]). The neural network improves the performance of contact tracing (to the level of the unrealistic a total lockdown) while performing the same number of tests and isolating the same fraction of the population. The neural network autonomously tunes its weights to the ongoing outbreak without needing to know the disease outbreak parameters and, since it is regularly retrained as new data become available, it will automatically adapt itself to the evolution

of the outbreak. As always, there is a possibility for improvement in the performance of the network, by providing it, for example, demographic and spatial information of the individuals.

Throughout my PhD studies, my research has been interdisciplinary in nature and has allowed me to apply new technologies developed in the field of physics to solve problems in the fields of biology and biomedicine. This kind of transfer of technology is something that I believe to be critical for the advancement of science in general. In order to lower the barrier for the uptake of new technologies in other fields it is important to work closely with the potential users to understand the challenges they face, something I feel like I have been lucky enough to do when collaborating with medical doctors and clinical specialists.

CHAPTER 4

Compilation of papers

4.1 Paper I: Digital video microscopy enhanced by deep learning

Attached is the full paper as published in Optica as well as its accompanying Supplementary Material that provides more details on the neural network architecture, training and inference, the training image generation, the experimental setups and bacteria preparation, the standard algorithms, the analysis methods, and the performance of DeepTrack for small close particles and the description of the codes provided.

4.2 Paper II: Quantitative digital microscopy with deep learning

Attached is the full paper as published in Applied Physics Reviews.

4.3 Paper III: Extracting quantitative biological information from brightfield cell images using deep learning

Attached is the preprint version of the paper as found on arXiv and its accompanying Supplementary material that provides more details on the results for 40× and 20× magnifications.

4.4 Paper IV: Virtual genetic diagnosis for familial hypercholesterolemia powered by machine learning

Attached is the full paper as published in the European Journal of Preventive Cardiology as well as its accompanying Supplementary material that provides more details on the study cohorts, the calculation of the clinical score, the preprocessing of the data, and the machine learning algorithms and their training, testing and evaluation.

4.5 Paper V: Enhanced prediction of atrial fibrillation and mortality among patients with congenital heart disease using big data and deep learning

Attached is the full manuscript that is under review in the European Heart Journal – Digital Health as well as its accompanying Supplementary material that provides more details on the data preprocessing, the neural network training, testing and evaluation, the congenital heart disease lesion groups and baseline characteristics of the patients, and the full breakdown of the results.

4.6 Paper VI: Improving epidemic testing and containment strategies using machine learning

Attached is the full manuscript accepted for publication Machine Learning: Science and Technology as well as its accompanying Supplementary Material that provides more details on the motivation for the parameters of the SIR model employed, the quality of the neural network as a binary classification problem, and three additional examples of testing strategies alternative to the standard contact-tracing strategy.

Bibliography

1. Chollet, F. *Deep learning with Python* (Manning New York, 2018).
2. Mehlig, B. *Machine learning with neural networks* 2021. arXiv: 1901.05639.
3. Rumelhart, D. E., Hinton, G. E. & Williams, R. J. Learning representations by back-propagating errors. *Nature* **323,** 533–536 (1986).
4. LeCun, Y. *et al.* Backpropagation applied to handwritten zip code recognition. *Neural Computation* **1,** 541–551 (1989).
5. Krizhevsky, A., Sutskever, I. & Hinton, G. E. Imagenet classification with deep convolutional neural networks. *Advances in Neural Information Processing Systems* **25,** 1097–1105 (2012).
6. Deng, J. *et al. Imagenet: A large-scale hierarchical image database* in *2009 IEEE Conference on Computer Vision and Pattern Recognition* (2009), 248–255.
7. LeCun, Y., Bengio, Y. & Hinton, G. Deep learning. *Nature* **521,** 436–444 (2015).
8. Ronneberger, O., Fischer, P. & Brox, T. *U-net: Convolutional networks for biomedical image segmentation* in *International Conference on Medical Image Computing and Computer Assisted Intervention* (2015), 234–241.
9. Goodfellow, I. J. *et al. Generative Adversarial Networks* 2014. arXiv: 1406.2661.
10. Hannel, M. D., Abdulali, A., O'Brien, M. & Grier, D. G. Machine-learning techniques for fast and accurate feature localization in holograms of colloidal particles. *Optics Express* **26,** 15221–15231 (2018).
11. Newby, J. M., Schaefer, A. M., Lee, P. T., Forest, M. G. & Lai, S. K. Convolutional neural networks automate detection for tracking of submicron-scale particles in 2D and 3D. *Proceedings of the National Academy of Sciences* **115,** 9026–9031 (2018).
12. Helgadottir, S., Argun, A. & Volpe, G. Digital video microscopy enhanced by deep learning. *Optica* **6,** 506–513 (2019).

13. Midtvedt, B. *et al.* Quantitative digital microscopy with deep learning. *Applied Physics Reviews* **8,** 011310 (2021).

14. Midtvedt, B. *et al.* Fast and Accurate Nanoparticle Characterization Using Deep-Learning-Enhanced Off-Axis Holography. *ACS Nano.*

15. Wu, Y. *et al.* Extended depth-of-field in holographic imaging using deep-learning-based autofocusing and phase recovery. *Optica* **5,** 704–710 (2018).

16. Altman, L. E. & Grier, D. G. CATCH: Characterizing and tracking colloids holographically using deep neural networks. *The Journal of Physical Chemistry B* **124,** 1602–1610 (2020).

17. Nehme, E., Weiss, L. E., Michaeli, T. & Shechtman, Y. Deep-STORM: super-resolution single-molecule microscopy by deep learning. *Optica* **5,** 458–464 (2018).

18. Ouyang, W., Aristov, A., Lelek, M., Hao, X. & Zimmer, C. Deep learning massively accelerates super-resolution localization microscopy. *Nature Biotechnology* **36,** 460–468 (2018).

19. Jeon, W., Jeong, W., Son, K. & Yang, H. Speckle noise reduction for digital holographic images using multi-scale convolutional neural networks. *Optics Letters* **43,** 4240–4243 (2018).

20. Choi, G. *et al.* Cycle-consistent deep learning approach to coherent noise reduction in optical diffraction tomography. *Optics Express* **27,** 4927–4943 (2019).

21. Wu, Y. *et al.* Bright-field holography: cross-modality deep learning enables snapshot 3D imaging with bright-field contrast using a single hologram. *Light: Science & Applications* **8,** 1–7 (2019).

22. Zhou, S. K. *et al.* A review of deep learning in medical imaging: Imaging traits, technology trends, case studies with progress highlights, and future promises. *Proceedings of the IEEE* (2021).

23. Moen, E. *et al.* Deep learning for cellular image analysis. *Nature Methods* **16,** 1233–1246 (2019).

24. Falk, T. *et al.* U-Net: deep learning for cell counting, detection, and morphometry. *Nature Methods* **16,** 67–70 (2019).

25. Sadanandan, S. K., Ranefall, P., Le Guyader, S. & Wählby, C. Automated training of deep convolutional neural networks for cell segmentation. *Scientific Reports* **7,** 1–7 (2017).

26. Xie, W., Noble, J. A. & Zisserman, A. Microscopy cell counting and detection with fully convolutional regression networks. *Computer Methods in Biomechanics and Biomedical Engineering: Imaging & Visualization* **6,** 283–292 (2018).

27. Campanella, G. *et al.* Clinical-grade computational pathology using weakly supervised deep learning on whole slide images. *Nature Medicine* **25,** 1301–1309 (2019).

28. Echle, A. *et al.* Deep learning in cancer pathology: a new generation of clinical biomarkers. *British Journal of Cancer,* 1–11 (2020).

29. Wieslander, H. *et al.* Deep learning with conformal prediction for hierarchical analysis of large-scale whole-slide tissue images. *IEEE Journal of Biomedical and Health Informatics* **25,** 371–380 (2020).

30. Helgadottir, S. *et al. Extracting quantitative biological information from brightfield cell images using deep learning* 2020. arXiv: 2012.12986.

31. Rivenson, Y. *et al.* PhaseStain: the digital staining of label-free quantitative phase microscopy images using deep learning. *Light: Science & Applications* **8,** 1–11 (2019).

32. Rivenson, Y. *et al.* Virtual histological staining of unlabelled tissue-autofluorescence images via deep learning. *Nature Biomedical Engineering* **3,** 466–477 (2019).

33. Christiansen, E. M. *et al.* In silico labeling: predicting fluorescent labels in unlabeled images. *Cell* **173,** 792–803 (2018).

34. Li, X. *et al.* Unsupervised content-preserving transformation for optical microscopy. *Light: Science & Applications* **10,** 1–11 (2021).

35. Cheng, S. *et al.* Single-cell cytometry via multiplexed fluorescence prediction by label-free reflectance microscopy. *Science Advances* **7,** eabe0431 (2021).

36. Imboden, S. *et al.* Investigating heterogeneities of live mesenchymal stromal cells using AI-based label-free imaging. *Scientific Reports* **11,** 1–11 (2021).

37. Ching, T. *et al.* Opportunities and obstacles for deep learning in biology and medicine. *Journal of The Royal Society Interface* **15,** 20170387 (2018).

38. Miotto, R., Wang, F., Wang, S., Jiang, X. & Dudley, J. T. Deep learning for healthcare: review, opportunities and challenges. *Briefings in Bioinformatics* **19,** 1236–1246 (2018).

39. Bakator, M. & Radosav, D. Deep learning and medical diagnosis: A review of literature. *Multimodal Technologies and Interaction* **2,** 47 (2018).

40. Pina, A. *et al.* Virtual genetic diagnosis for familial hypercholesterolemia powered by machine learning. *European Journal of Preventive Cardiology* **27,** 1639–1646 (2020).

41. Yanase, J. & Triantaphyllou, E. A systematic survey of computer-aided diagnosis in medicine: Past and present developments. *Expert Systems with Applications* **138,** 112821 (2019).

42. Perrin, J. Mouvement brownien et molécules. *Journal of Physics: Theories and Applications* **9,** 5–39 (1910).

43. Crocker, J. C. & Grier, D. G. Methods of digital video microscopy for colloidal studies. *Journal of Colloid and Interface Science* **179,** 298–310 (1996).

44. Parthasarathy, R. Rapid, accurate particle tracking by calculation of radial symmetry centers. *Nature Methods* **9,** 724–726 (2012).

45. Xing, F., Xie, Y., Su, H., Liu, F. & Yang, L. Deep learning in microscopy image analysis: A survey. *IEEE Transactions on Neural Networks and Learning Systems* **29,** 4550–4568 (2017).

46. Lulevich, V., Shih, Y.-P., Lo, S. H. & Liu, G.-y. Cell tracing dyes significantly change single cell mechanics. *The Journal of Physical Chemistry B* **113,** 6511–6519 (2009).

47. Alford, R. *et al.* Toxicity of organic fluorophores used in molecular imaging: literature review. *Molecular Imaging* **8,** 7290–2009 (2009).

48. Zhang, Y. *et al.* Digital synthesis of histological stains using micro-structured and multiplexed virtual staining of label-free tissue. *Light: Science & Applications* **9,** 1–13 (2020).

49. Nygate, Y. N. *et al.* Holographic virtual staining of individual biological cells. *Proceedings of the National Academy of Sciences* **117,** 9223–9231 (2020).

50. Ounkomol, C., Seshamani, S., Maleckar, M. M., Collman, F. & Johnson, G. R. Label-free prediction of three-dimensional fluorescence images from transmitted-light microscopy. *Nature Methods* **15,** 917–920 (2018).

51. Li, D. *et al.* Deep learning for virtual histological staining of bright-field microscopic images of unlabeled carotid artery tissue. *Molecular Imaging and Biology* **22,** 1301–1309 (2020).

52. Liu, Y., Yuan, H., Wang, Z. & Ji, S. Global pixel transformers for virtual staining of microscopy images. *IEEE Transactions on Medical Imaging* **39,** 2256–2266 (2020).

53. McQuin, C. *et al.* CellProfiler 3.0: Next-generation image processing for biology. *PLOS Biology* **16,** e2005970 (2018).

54. Rudin, C. Stop explaining black box machine learning models for high stakes decisions and use interpretable models instead. *Nature Machine Intelligence* **1,** 206–215 (2019).

55. Nordestgaard, B. G. *et al.* Familial hypercholesterolaemia is underdiagnosed and undertreated in the general population: guidance for clinicians to prevent coronary heart disease: consensus statement of the European Atherosclerosis Society. *European Heart Journal* **34,** 3478–3490 (2013).

56. Wierzbicki, A. S., Humphries, S. E. & Minhas, R. Familial hypercholesterolaemia: summary of NICE guidance. *BMJ* **337** (2008).

57. Maglio, C. *et al.* Genetic diagnosis of familial hypercholesterolaemia by targeted next-generation sequencing. *Journal of Internal Medicine* **276,** 396–403 (2014).

58. Hegele, R. A. *et al.* Targeted next-generation sequencing in monogenic dyslipidemias. *Current Opinion in Lipidology* **26,** 103–113 (2015).

59. Benn, M., Watts, G. F., Tybjaerg-Hansen, A. & Nordestgaard, B. G. Familial hypercholesterolemia in the Danish general population: prevalence, coronary artery disease, and cholesterol-lowering medication. *The Journal of Clinical Endocrinology & Metabolism* **97,** 3956–3964 (2012).

60. Defesche, J. C., Lansberg, P. J., Umans-Eckenhausen, M. A. & Kastelein, J. J. *Advanced method for the identification of patients with inherited hypercholesterolemia* in *Seminars in Vascular Medicine* **4** (2004), 59–65.

61. Casula, M. *et al.* Evaluation of the performance of Dutch Lipid Clinic Network score in an Italian FH population: The LIPIGEN study. *Atherosclerosis* **277,** 413–418 (2018).

62. Hoffman, J. I. & Kaplan, S. The incidence of congenital heart disease. *Journal of the American college of cardiology* **39,** 1890–1900 (2002).

63. Khoshnood, B. *et al.* Prevalence, timing of diagnosis and mortality of newborns with congenital heart defects: a population-based study. *Heart* **98,** 1667–1673 (2012).

64. Botto, L. D., Lin, A. E., Riehle-Colarusso, T., Malik, S. & Correa, A. Seeking causes: classifying and evaluating congenital heart defects in etiologic studies. *Birth Defects Research Part A: Clinical and Molecular Teratology* **79,** 714–727 (2007).

65. Liu, S. *et al.* Effect of folic acid food fortification in Canada on congenital heart disease subtypes. *Circulation* **134,** 647–655 (2016).

66. Flaxman, S. *et al.* Estimating the effects of non-pharmaceutical interventions on COVID-19 in Europe. *Nature* **584,** 257–261 (2020).

67. Giordano, G. *et al.* Modelling the COVID-19 epidemic and implementation of population-wide interventions in Italy. *Nature Medicine* **26,** 855–860 (2020).

68. Lavezzo, E. *et al.* Suppression of a SARS-CoV-2 outbreak in the Italian municipality of Vo'. *Nature* **584,** 425–429 (2020).

69. Aleta, A. *et al.* Modelling the impact of testing, contact tracing and household quarantine on second waves of COVID-19. *Nature Human Behaviour* **4,** 964–971 (2020).

70. Navascues, M., Budroni, C. & Guryanova, Y. *Disease control as an optimization problem* 2021. arXiv: 2009.06576.

71. Wang, L., Lin, Z. Q. & Wong, A. Covid-net: A tailored deep convolutional neural network design for detection of covid-19 cases from chest x-ray images. *Scientific Reports* **10,** 1–12 (2020).

72. Dandekar, R. & Barbastathis, G. *Neural Network aided quarantine control model estimation of global Covid-19 spread* 2020. arXiv: 2004.02752.

73. Lalmuanawma, S., Hussain, J. & Chhakchhuak, L. Applications of machine learning and artificial intelligence for Covid-19 (SARS-CoV-2) pandemic: A review. *Chaos, Solitons & Fractals,* 110059 (2020).

74. Natali, L., Helgadottir, S., Marago, O. M. & Volpe, G. Improving epidemic testing and containment strategies using machine learning. *Machine Learning: Science and Technology* (accepted 2021).

75. Kermack, W. O. & McKendrick, A. G. A contribution to the mathematical theory of epidemics. *Proceedings of the Royal Society of London. Series A, Containing Papers of a Mathematical and Physical Character* **115,** 700–721 (1927).

76. Weiss, H. H. The SIR model and the foundations of public health. *Materials Matematics,* 0001–17 (2013).

77. Liu, L. *et al.* Deep learning for generic object detection: A survey. *International Journal of Computer Vision* **128,** 261–318 (2020).

78. Perrone, M. P. & Cooper, L. N. *When networks disagree: Ensemble methods for hybrid neural networks* tech. rep. (BROWN UNIV PROVIDENCE RI INST FOR BRAIN and NEURAL SYSTEMS, 1992).

79. Chenouard, N. *et al.* Objective comparison of particle tracking methods. *Nature Methods* **11,** 281–289 (2014).

80. Helgadottir, S., Argun, A. & Volpe, G. *DeepTrack-1.0* https://github.com/softmatterlab/DeepTrack. 2019.

81. Fränzl, M. & Cichos, F. Active particle feedback control with a single-shot detection convolutional neural network. *Scientific Reports* **10,** 1–7 (2020).

82. Franchini, S. & Krevor, S. Cut, overlap and locate: a deep learning approach for the 3D localization of particles in astigmatic optical setups. *Experiments in Fluids* **61,** 1–15 (2020).

83. Oktay, A. B. & Gurses, A. Automatic detection, localization and segmentation of nano-particles with deep learning in microscopy images. *Micron* **120,** 113–119 (2019).

84. Helgadottir, S., Argun, A. & Volpe, G. Deep Learning for Particle Tracking. *Optics & Photonics News, "Optics in 2019"* (2019).

85. LeCun, Y., Cortes, C. & Burges, C. MNIST handwritten digit database. *ATT Labs [Online]. Available: http://yann.lecun.com/exdb/mnist* **2** (2010).

86. Gerhard, S., Funke, J., Martel, J., Cardona, A. & Fetter, R. Segmented anisotropic ssTEM dataset of neural tissue. *figshare* (2013).

87. Causley, D. & Young, J. Z. Counting and sizing of particles with the flying-spot microscope. *Nature* **176,** 453–454 (1955).

88. Midtvedt, B. *et al. DeepTrack-2.0* https://github.com/softmatterlab/DeepTrack-2.0. 2020.

89. Midtvedt, B. *et al. DeepTrack-2.0-app* https://github.com/softmatterlab/DeepTrack-2.0-app. 2020.

90. Schindelin, J. *et al.* Fiji: an open-source platform for biological-image analysis. *Nature Methods* **9,** 676–682 (2012).

91. Midtvedt, B. *et al.* Partikelanalys och mikroskopi - från Einstein till neurala nätverk. *Fysikaktuellt* **20,** 17 (2021).

92. Yanina, I. Y., Lazareva, E. N. & Tuchin, V. V. Refractive index of adipose tissue and lipid droplet measured in wide spectral and temperature ranges. *Applied Optics* **57,** 4839–4848 (2018).

93. Schürmann, M., Scholze, J., Müller, P., Guck, J. & Chan, C. J. Cell nuclei have lower refractive index and mass density than cytoplasm. *Journal of Biophotonics* **9,** 1068–1076 (2016).

94. Helgadottir, S., Midtvedt, B., Pineda, J., Midtvedt, D. & Volpe, G. *VirtualStaining* https://github.com/softmatterlab/VirtualStaining, 2020.

95. Banda, J. M. *et al.* Finding missed cases of familial hypercholesterolemia in health systems using machine learning. *NPJ Digital Medicine* **2,** 1–8 (2019).

96. Besseling, J. *et al.* Selection of individuals for genetic testing for familial hypercholesterolaemia: development and external validation of a prediction model for the presence of a mutation causing familial hypercholesterolaemia. *European Heart Journal* **38,** 565–573 (2017).

97. Helgadottir, S., Volpe, G. & Romeo, S. Diagnostisering av sjukdomar förbättras med maskininlärning. *Fysikaktuellt* **19,** 15 (2020).

98. Mandalenakis, Z. *et al.* Survivorship in children and young adults with congenital heart disease in Sweden. *JAMA Internal Medicine* **177,** 224–230 (2017).

99. Moons, P., Bovijn, L., Budts, W., Belmans, A. & Gewillig, M. Temporal trends in survival to adulthood among patients born with congenital heart disease from 1970 to 1992 in Belgium. *Circulation* **122,** 2264–2272 (2010).

100. Van der Bom, T. *et al.* Contemporary survival of adults with congenital heart disease. *Heart* **101,** 1989–1995 (2015).

101. Diller, G.-P. *et al.* Machine learning algorithms estimating prognosis and guiding therapy in adult congenital heart disease: data from a single tertiary centre including 10 019 patients. *European Heart Journal* **40,** 1069–1077 (2019).

102. Mandalenakis, Z. *et al.* Survival in Children with congenital heart disease: Have we reached a peak at 97%? *Journal of the American Heart Association* **9,** e017704 (2020).

103. Kiang, R. *et al.* Meteorological, environmental remote sensing and neural network analysis of the epidemiology of malaria transmission in Thailand. *Geospatial Health,* 71–84 (2006).

104. Augusta, C., Deardon, R. & Taylor, G. Deep learning for supervised classification of spatial epidemics. *Spatial and Spatio-temporal Epidemiology* **29,** 187–198 (2019).

105. Melin, P., Monica, J. C., Sanchez, D. & Castillo, O. *Multiple ensemble neural network models with fuzzy response aggregation for predicting COVID-19 time series: the case of Mexico* in *Healthcare* **8** (2020), 181.

106. Park, Y. J. *et al.* Contact tracing during coronavirus disease outbreak, South Korea, 2020. *Emerging Infectious Diseases* **26,** 2465–2468 (2020).

107. Kretzschmar, M. E. *et al.* Impact of delays on effectiveness of contact tracing strategies for COVID-19: a modelling study. *The Lancet Public Health* **5,** e452–e459 (2020).

108. Keeling, M. J. & Rohani, P. *Modeling infectious diseases in humans and animals* (Princeton university press, 2011).

109. Black, A. J. & McKane, A. J. Stochastic formulation of ecological models and their applications. *Trends in Ecology & Evolution* **27,** 337–345 (2012).

110. Ferretti, L. *et al.* Quantifying SARS-CoV-2 transmission suggests epidemic control with digital contact tracing. *Science* **368** (2020).

111. Clipman, S. J. *et al.* Rapid Real-time Tracking of Nonpharmaceutical Interventions and Their Association With Severe Acute Respiratory Syndrome Coronavirus 2 (SARS-CoV-2) Positivity: The Coronavirus Disease 2019 (COVID-19) Pandemic Pulse Study. *Clinical Infectious Diseases* (2020).

112. Long, Q.-X. *et al.* Clinical and immunological assessment of asymptomatic SARS-CoV-2 infections. *Nature Medicine* **26,** 1200–1204 (2020).

113. Seow, J. *et al.* Longitudinal observation and decline of neutralizing antibody responses in the three months following SARS-CoV-2 infection in humans. *Nature Microbiology* **5,** 1598–1607 (2020).

114. Shaman, J. & Galanti, M. Will SARS-CoV-2 become endemic? *Science* **370,** 527–529 (2020).

115. Chinazzi, M. *et al.* The effect of travel restrictions on the spread of the 2019 novel coronavirus (COVID-19) outbreak. *Science* **368,** 395–400 (2020).

Acknowledgements

First and foremost I would like to thank my amazing research group, a group of the most kind, smart and helpful people. I would also like to thank my supervisor Giovanni Volpe for giving me all the opportunities and tools to succeed.